Robustness of first-order phase transitions in one-dimensional long-range contact processes

Carlos E. Fiore and Mário J. de Oliveira
Departamento de Física, Universidade Federal do Paraná, Caixa Postal 19044, 81531-000 Curitiba, Paraná, Brazil, and Instituto de Física, Universidade de São Paulo, Caixa Postal 66318, 05315-970 São Paulo, Brazil
(Received 24 November 2012; published 3 April 2013)

It has been proposed [Ginelli *et al.*, Phys. Rev. E **71**, 026121 (2005)] that, unlike the short-range contact process, the long-range counterpart may lead to the existence of a discontinuous phase transition in one dimension. Aiming to explore such a link, here we investigate thoroughly a family of long-range contact processes. They are introduced through the transition rate $1 + a\ell^{-\sigma}$, where ℓ is the length of inactive islands surrounding particles. In the former approach we reconsider the original model (called the σ-contact process) by considering distinct mechanisms of weakening the long-range interaction toward the short-range limit. In addition, we study the effect of different rules, including creation and annihilation by clusters of particles and distinct versions with infinitely many absorbing states. Our results show that for all examples presenting a single absorbing state, a discontinuous transition is possible for small σ. On the other hand, the presence of infinite absorbing states leads to a distinct scenario depending on the interactions at the perimeter of inactive sites.

DOI: 10.1103/PhysRevE.87.042101 PACS number(s): 05.70.Ln, 05.50.+q, 05.65.+b

I. INTRODUCTION

Nonequilibrium phase transitions into absorbing states describe a large assortment of phenomena including chemical reactions, spreading of disease, competition between species, wetting processes, calcium dynamics, and others [1,2]. Due to the lack of analogous examples in equilibrium statistical mechanics, they are essential in the establishment of the main ingredients required for the emergence of phase transitions and critical behavior.

The contact process (CP) [3] is probably the best example yielding an absorbing phase transition. Particles are created catalytically but are spontaneously annihilated. This presents a set of critical exponents belonging to the directed percolation (DP) universality class. The DP conjecture [4] embraces not only the CP, but also generic absorbing phase transitions with no extra symmetries and conservation laws. Examples are reaction-diffusion processes, cellular automata models, and even continuous descriptions with multiplicative noise [5,6]. More recently it has been observed experimentally in turbulent nematic liquid crystals [7].

Differently from the continuous case, one-dimensional discontinuous absorbing transitions have been much less observed. Except in special cases [8–10], their manifestation in short-range systems has been the subject of a long-standing controversy [11–15]. The absence of a discontinuous transition would stem from the suppression of compact clusters coming from large fluctuations in one dimension. On the other hand, upon increasing the dimensionality, the fluctuations are less relevant and the formation of compact clusters becomes possible.

Long-range interactions have been proposed as more realistic descriptions in different nonequilibrium phenomena, compared with their short-range counterparts. Some examples of systems presenting long-range interactions include wetting phenomena, spreading of diseases over long distances and others [16–18]. As an effect of long-range interactions, the absorbing transition may deviate from the original DP case and belong to different universality classes [19–24]. Another remarkable difference concerns the possibility of stabilizing compact clusters in one dimension. Ginelli *et al.* [25] introduced the σ-CP, in which particles are created and annihilated as in the usual short-range CP, but the activation rate depends on the length ℓ of the island of inactive sites according to the expression $1 + a\ell^{-\sigma}$. They found that for $0 < \sigma < 1$ the interactions are effectively long-range and the phase transition becomes discontinuous. On the other hand, for $\sigma > 1$ the long-range parameter does not play a relevant role and the phase transition remains second order (similar to its short-range version).

Despite the study of the σ-CP under different methodologies [25,26], some aspects have not been addressed so far. Is a first-order transition in the limit of extremely weak ($a \ll 1$) long-range interactions present? Does the competition with short-range interactions leave the system still able to suppress fluctuations that destabilize compact clusters? Is the phase coexistence maintained by changing the interaction rules? and Does the existence of infinitely absorbing states influence the order of transition?

Aiming to answer these queries, in this paper we investigate thoroughly a family of one-dimensional long-range contact models. First, we reconsider the σ-CP by weakening sufficiently the long-range interaction toward the short-range limit and, further, by introducing an effective competition with short-range interactions. Although the emergence of a discontinuous transition is expected not to depend on the parameter a [25], a quite interesting point would concern the stabilization of compact clusters over extremely small long-range interactions (thus close to the short-range regime). In such cases the long-range interactions should act as a small (but relevant) perturbation. Second, we consider the effect of different interaction rules, including creation and annihilation in the presence of clusters of particles (instead of the one-particle case) and infinitely many absorbing states. These models are long-range versions of the named pair-creation CP, the pair-annihilation model (PAM), the triplet-annihilation model (TAM), and the pair CP (PCP) [11,27,28]. All models are studied over mean-field approximations and extensive numerical simulations in the constant-rate (ordinary)

[1] and the constant-particle-number (conserved) ensembles [26,29–32]. Our results show that for all systems with a single absorbing state the occurrence of discontinuous transitions is held by decreasing σ. For the long-range PCP, on the other hand, different scenarios are possible. By measuring the length ℓ between extreme pairs of particles, the transition becomes first order for low σ. On the other hand, when ℓ is the distance between a pair and the nearest particle surrounding the inactive island, the transition is always continuous.

This paper is organized as follows: In Sec. II we describe all the methods, in Sec. III we present the models and numerical results, and finally, conclusions are presented in Sec. IV.

II. CONSTANT RATE AND CONSERVED ENSEMBLES

The one-dimensional CP is defined in a chain of L sites where each site i is attached by a two-state occupation variable η_i reading $\eta_i = 0$ or 1, according to whether it is empty or occupied, respectively. Interaction rules are composed of creation and annihilation of particles, represented by transition rates ω_i^c and ω_i^a. Particles are created in empty active sites and are spontaneously annihilated.

Systems are studied in the constant-rate (ordinary) and in the constant-particle-number (conserved) ensembles [26,29, 31,32]. In the former case the control parameters (creation or annihilation rates) are held fixed but the total particle number $\bar{n}$ fluctuates. It is described by the total transition rate w_i,

$$w_i = \omega_i^c + \alpha\omega_i^a, \tag{1}$$

where α denotes the strength of the annihilation rate. For low α, the phase is active, and particles are continuously created and annihilated. Upon an increase in α, a phase transition into an absorbing state takes place. Except for the PCP, the absorbing state is characterized by a full empty lattice. For the PCP, any configuration devoid of pairs is absorbing.

The transition point and the nature of transition can be precisely identified by performing spreading simulations [1]. Starting from an initial seed, this consists of determining the time evolution of appropriate quantities, such as the survival probability $P_s(t)$, the total number of particles $N(t)$, and the mean square spreading $R^2(t)$.

At the emergence of the phase transition, these quantities follow algebraic behaviors given by

$$P_s(t) \sim t^{-\delta}, \quad N(t) \sim t^{\eta}, \quad \text{and} \quad R^2(t) \sim t^{2/z}, \tag{2}$$

where δ, η, and z are their associated dynamic critical exponents. For second-order DP phase transitions, they read $\delta = 0.159\,464(6)$, $\eta = 0.313\,686(8)$, and $z = 1.580\,745(10)$ [6]. In a discontinuous transition, despite the order parameter gap, they also present algebraic behaviors, with critical exponents given by $\delta = 1/2$, $\eta = 0$, and $z = 1$, which is compatible with the Glauber-Ising (GI) model [6].

Thus, spreading simulations can not only locate the transition point, but also classify the order of transition. A change in the order of transition will be characterized by an alteration of the critical exponents. Off the transition regime, the above dynamic quantities deviate from power-law behaviors.

For systems with infinitely many absorbing states [33], spreading experiments become particularly hard to use. In particular, the dynamic exponents δ, η, and z are strongly dependent on the initial conditions, presenting nonuniversal values [33–36]. A simpler procedure for locating the critical point in such cases is to study the order-parameter decay starting from a fully occupied initial condition. Unlike the above exponents, θ does not depend on the initial configuration. One expects ϕ to behave as $\phi \sim t^{-\theta}$ at the critical point, where $\theta = \delta$. Conversely, we should expect a non-power-law behavior at a discontinuous transition. Since alternative methods (e.g., hysteretic ones) cannot be used for systems with absorbing states, another strategy is required. In particular, we have calculated the probability distribution (in the steady regime) by considering different initial configurations. A bimodal distribution reveals the discontinuous transition.

In the constant-rate ensemble, the control parameter is the total particle number n. Particles are created as in the ordinary case, but instead of creating new particles, a cluster of k sites leaves its place and jumps to k active sites. One may define the conserved ensemble as a $2k$-site process, in which creation and annihilation occur simultaneously according to the following transition [32]:

$$w = \omega_i^a \underbrace{\omega_j^c\omega_l^c \ldots \omega_m^c}_{k\text{-creation processes}} . \tag{3}$$

It has been shown [31,32] that in the thermodynamic limit the above dynamics is equivalent to that studied in the constant-rate ensemble. The parameter $\bar{\alpha}$ fluctuates and is calculated through the expression

$$\bar{\alpha} = \frac{\langle\omega_j^c\rangle_c}{k\langle\omega_i^a\rangle_c}, \tag{4}$$

where $\langle\cdots\rangle_c$ denotes a generic average evaluated over the conserved ensemble. An immediate advantage concerns its simplicity for locating the transition point. In this case, by considering a system constrained in the subcritical regime, e.g, a finite number of particles placed in an infinite lattice, the addition of particles drives the system toward the transition point α_0 according to the expression [26,29,32,37]

$$\bar{\alpha} - \alpha_0 \sim n^{-1}. \tag{5}$$

Thus, from the above, the transition point is obtained by linear extrapolation in $1/n$. Another advantage refers to the classification of the phase transition, obtained by measuring the particle structures for different n values. For second-order transitions, the clusters are fractals [38], whereas they become compact in a discontinuous transition. With R being the mean distance of particles located at extremities of the system, we have that [1,26,32]

$$R \sim n^{1/d_F}, \tag{6}$$

where d_F is the fractal dimension. For one-dimensional systems belonging to the DP universality class d_F reads $0.74792\ldots$, whereas at phase coexistence it is the proper euclidean dimension $d = 1$ (consistent with the existence of compact clusters). The above values are related to the dynamic exponents through the expression $d_F = 2(\eta + \delta)/z$.

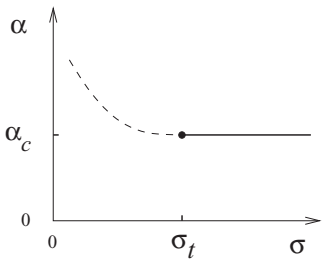

FIG. 1. Pair mean-field approximation phase diagram in space α versus σ. Solid and dashed lines denote second- and first-order phase transitions, respectively, and the filled circle denotes the tricritical point.

III. MEAN-FIELD APPROXIMATION

Before performing simulations we analyzed the models by means of a cluster approximation at the level of two nearest-neighbor sites [26]. In this case, the system is described by the one-site probabilities $P(0)$ and $P(1)$ and the two-site probabilities $P(11)$, $P(10)$, $P(01)$, and $P(11)$. However, only two of them are independent. The generic probability of a string of ℓ consecutive sites is approximated by

$$P(\eta_1,\eta_2,\eta_3,\ldots,\eta_\ell)=\frac{P(\eta_1,\eta_2)P(\eta_2,\eta_3)\cdots P(\eta_{\ell-1},\eta_\ell)}{P(\eta_2)P(\eta_3)\cdots P(\eta_{\ell-1})}. \tag{7}$$

By choosing $P(1)=\langle\eta_i\rangle$ and $P(11)=\langle\eta_i\eta_{i+1}\rangle$ and taking into account the translation invariance, their evolution equations read

$$\frac{d}{dt}\langle\eta_i\rangle=\langle(\bar\eta_i-\eta_i)w_i(\eta)\rangle \tag{8}$$

and

$$\frac{d}{dt}\langle\eta_i\eta_{i+1}\rangle=\langle(\bar\eta_i-\eta_i)\eta_{i+1}w_i(\eta)\rangle + \langle\eta_i(\bar\eta_{i+1}-\eta_{i+1})w_{i+1}(\eta)\rangle, \tag{9}$$

where $\bar\eta_i\equiv 1-\eta_i$. By using approximation (7), we get a set of two closed equations for $P(1)=\rho$ and $P(11)=\phi$. In the stationary state we found, for all models studied, a general structure in the relation for α vs ρ, given by

$$\alpha\rho=\alpha_c\rho+A\rho^2 \tag{10}$$

up to order ρ^2, where α_c is a numerical constant and A depends on the other parameters but not on α. From this equation it follows that a critical line occurs at $\alpha=\alpha_c$ and $A<0$. When $A>0$, the transition becomes first order and a tricritical point occurs at $A=0$. The phase diagram is of the type shown in Fig. 1.

IV. NUMERICAL RESULTS

Except for the PCP model, numerical simulations are performed for large system sizes ($L=2^{16}$) and periodic boundary conditions. In the conserved case, Monte Carlo simulations are started by constraining the system in the subcritical (absorbing) regime. In practice, it is done by taking finite ns in a large L and check whether a particle touches the border. If a particle reaches the border, we increase L. By simulating distinct ns [with $\bar\alpha$ computed from Eq. (5)], the transition point α_0 is obtained by means of a linear extrapolation in $1/n$. The nature of the phase transition is identified by calculating the fractal dimension, measured from the dependence of R on n. Further, we check the above results by performing epidemic simulations starting from an initial seed in which the transition point α_0 is located by identifying algebraic behaviors for N and P_s. Their corresponding dynamic exponents η and δ classify the order of transition.

A. Long-range contact process (σ-CP)

In the usual CP, particles are created in empty sites surrounded by at least one particle and are spontaneously annihilated. It is defined by the transition rates

$$\omega_i^c=\frac{1}{2}(1-\eta_i)\sum_\delta\eta_{i+\delta} \tag{11}$$

and

$$\omega_i^a=\eta_i, \tag{12}$$

for particle creation and annihilation, respectively. In the σ-CP the creation rate is replaced by the expression

$$\omega_i^c=\frac{1}{2}\sum_{\ell=1}^{\infty}\left(1+\frac{a}{\ell^\sigma}\right)\eta_{i-1}\bar\eta_i\bar\eta_{i+1}\cdots\bar\eta_{i+\ell-1}\eta_{i+\ell} +\frac{1}{2}\sum_{\ell=1}^{\infty}\left(1+\frac{a}{\ell^\sigma}\right)\eta_{i+1}\bar\eta_i\bar\eta_{i-1}\cdots\bar\eta_{i-\ell+1}\eta_{i-\ell}, \tag{13}$$

which depends on ℓ, a, and σ and $\bar\eta_i\equiv 1-\eta_i$. For $a=0$, one recovers the original short-range CP, whose second-order phase transition occurs at $\alpha_c=0.303227\ldots$ [1].

Here we have weakened the long-range interaction toward the short-range limit, in order to see if phase coexistence still exists for $a\ll 1$. In Fig. 2, we show results for $a=0.05$.

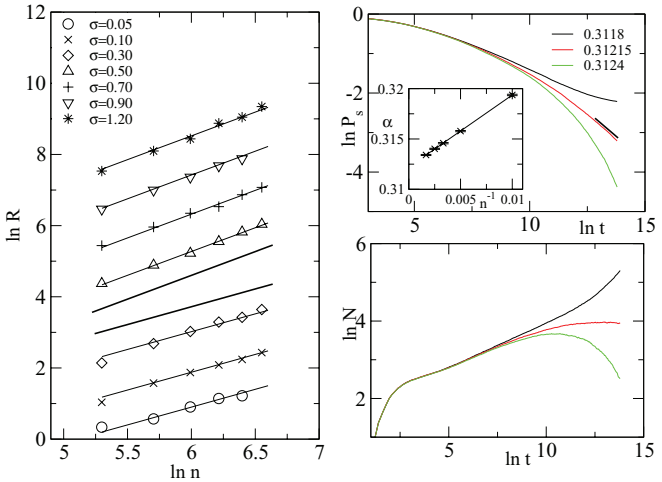

FIG. 2. (Color online) Left: Log-log plot of the average cluster size R versus the total number of particles n for several values of σ for $a=0.05$. The top and bottom predicted curves have slopes of 1.337 04 and 1, respectively. Data points have been shifted in order to avoid overlap. Right: Log-log plots of P_s (top) and N (bottom) for distinct values of α for $\sigma=0.1$. Predicted asymptotic slopes are consistent with GI values. Inset: Parameter $\bar\alpha$ versus n^{-1} in the conserved ensemble.

Note that the fractal dimension changes (from 0.75 to 1) for $\sigma < \sigma_t = 0.4(1)$, consistent with the emergence of a discontinuous transition for smaller σ. Spreading experiments, shown at the right for $\sigma = 0.1$, confirm this conclusion. At $\alpha_0 = 0.312\,15(5)$, both quantities, P_s and N, present algebraic behaviors consistent with exponents $\delta = 1/2$ and $\eta = 0$, respectively. The above estimate agrees very well with the conserved ensemble result, $\alpha_0 = 0.312\,21(3)$. In addition, we have also studied the possibility of discontinuous transitions for more extreme cases. For $a = 0.01$ and $\sigma = 0.005$, the transition is first order, yielding, at $\alpha_0 = 0.305\,72(3)$, a value rather close to the short-range case, 0.303 227. For completeness, we have considered the opposite case, e.g., the occurrence of discontinuous transition for larger a values. Our results (not shown) support that the first-order transition line moves toward larger σ values. For example, for $a = 5$ and $\sigma = 1.2$, the transition is first order, occurring at $\alpha_c = 0.439\,655(5)$. The crossover occurs at $\sigma_t = 1.3(1)$, which is larger than the $\sigma_t = 1.0(1)$ for $a = 2$.

The above conclusions are also predicted by pair mean-field results. They give a critical line at the value $\alpha_c = 1/2$ and a tricritical point occurring at

$$\zeta(\sigma_t) = \frac{1+a}{a}, \tag{14}$$

where $\zeta(\sigma)$ is the Riemann ζ function defined by $\zeta(\sigma) = \sum_{k=1}^{\infty} k^{-\sigma}$. From the above, it follows that $\sigma_t > 1$, in accordance with numerical results for larger a but not for sufficient small a values.

Further, we introduce the competition with short-range interactions. This is accomplished by performing short- and long-range process probabilities p and $1-p$, respectively. For low p, one expects qualitative behavior similar to that in the full long-range case, whereas for extremely large p, if a change in the transition occurs, it should manifest for a sufficiently low σ. In Fig. 3 we examine the phase transitions for $p = 0.98$ and different σ values. As in the previous

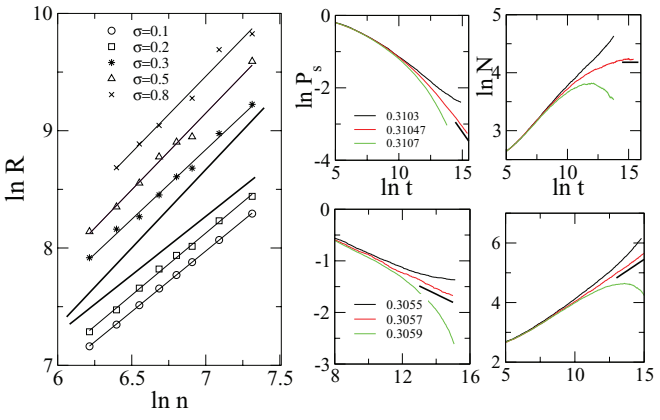

FIG. 3. (Color online) Left: Log-log plot of the average cluster size R versus the total number of particles n for several values of σ int the subcritical regime. Top and bottom straight lines have slopes of 1.337 04 and 1, respectively. Data points have been shifted in order to avoid overlap. Right: Log-log plots of the time evolution of P_s (left) and N (right) for distinct values of α for $\sigma = 0.1$ (top) and $\sigma = 0.3$ (bottom), respectively. Predicted asymptotic slopes are consistent with GI (top) and DP (bottom) values.

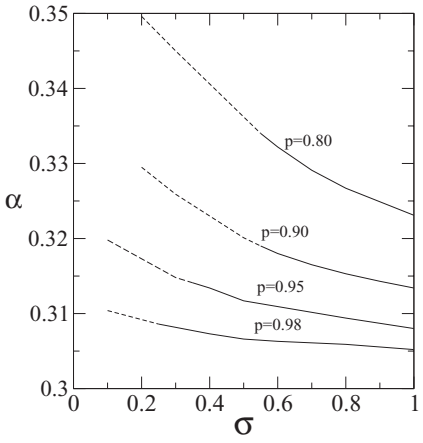

FIG. 4. Parameter α versus σ for different values of p. Solid and dashed lines denote second- and first-order transitions, respectively. For each p, absorbing and active phases are located above and below the corresponding lines, respectively.

case, the system structure also changes upon a decrease in σ and clusters become compact for $\sigma < 0.3$. This is also checked by comparing the time evolution of P_s and N for $\sigma = 0.3$ and $\sigma = 0.1$. At the transition points $\alpha_c = 0.3057(1)$ and $\alpha_0 = 0.310\,45(5)$, the above quantities present distinct algebraic behaviors consistent with the DP and GI exponents. In Fig. 4 we show the phase diagram for distinct (but large) values of p. As expected, the coexistence line moves toward lower values of σ.

In summary, the above "weakening" approaches show that a small long-range "perturbation" in the original CP suffices to provoke a change in the order of transition.

B. Long-range pair creation, pair- and triplet-annihilation contact models

Here we study the effect of distinct interaction rules on the long-range CP. The first change, called the σ-pair CP, is similar to the σ-CP, but new particles can be created only in empty sites surrounded by pairs of particles. The creation rate ω_i^c reads

$$\omega_i^c = \frac{1}{2}\sum_{\ell=1}^{\infty}\left(1+\frac{a}{\ell^\sigma}\right)\eta_{i-2}\eta_{i-1}\bar{\eta}_i\bar{\eta}_{i+1}\cdots\bar{\eta}_{i+\ell-1}\eta_{i+\ell} + \frac{1}{2}\sum_{\ell=1}^{\infty}\left(1+\frac{a}{\ell^\sigma}\right)\eta_{i+2}\eta_{i+1}\bar{\eta}_i\bar{\eta}_{i-1}\cdots\bar{\eta}_{i-\ell+1}\eta_{i-\ell}. \tag{15}$$

The limit $a = 0$ corresponds to the short-range pair-creation contact model case, in which a DP phase transition occurs at $\alpha_c = 0.133\,97(4)$ [32]. In Fig. 5, we show the main results for distinct σ values and $a = 2$. The transition is also continuous for $\sigma > 1$ and becomes first order for $0 < \sigma < 1$. However, as an effect of the creation in the presence of pairs, the clusters are somewhat more compact than the usual σ-CP. For example, for $\sigma = 0.5$ the cluster density $\rho = N/R$ (evaluated from the inverse of the slopes of curves R vs n) is about 0.78 for the σ-CP, whereas it reads 0.81 for the σ-pair CP. However, the creation

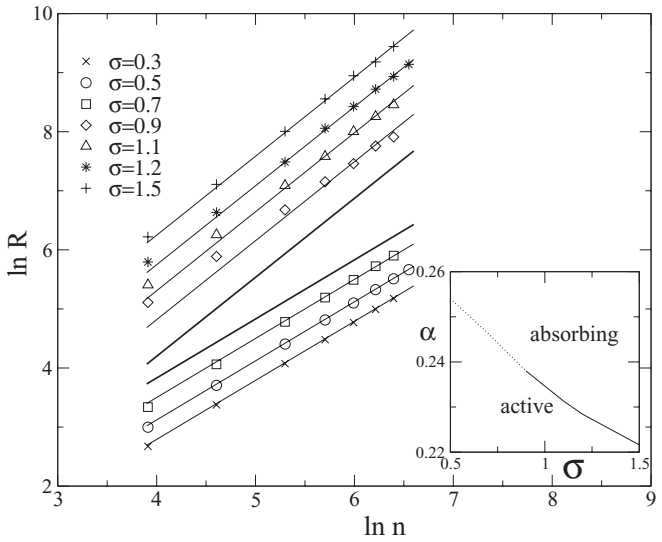

FIG. 5. Log-log plot of R versus n for the long-range pair-creation CP for distinct values of σ. The top and bottom straight lines have slopes of 1.337 04 and 1, respectively, and they have been shifted in order to avoid overlap. Inset: Phase diagram. Solid and dotted lines denote continuous and discontinuous transitions, respectively.

by pairs of particles is not sufficiently effective to shift the coexistence line for larger σ. In contrast to the σ-CP, the above results are not predicted by the pair mean-field approximation, in which the phase transition is always first order. On the other hand, when $\sigma \to \infty$ the parameter $\alpha \to 1/4$, which is in accordance with the mean-field short-range case.

Next, we consider the opposite situation, in which particles are created as in the above σ-CP, but only pairs of particles are allowed to be annihilated. The annihilation rate ω_i^a reads

$$\omega_i^a = \eta_i \eta_{i+1}. \tag{16}$$

Equation (4) is used to calculate $\bar{\alpha}$ in the conserved ensemble for $k = 2$. For $a = 0$ one recovers the original PAM, in which a DP continuous phase transition occurs at $\alpha_c = 0.186\,22(3)$ [27,32].

Like the σ-CP, for $a = 2$ the phase transition becomes first order for $0 < \sigma < 1$. The crossover between continuous and discontinuous occurs between 0.8 and 1.1. In Fig. 6 we show the main results for distinct σ values. As a consequence of the pair annihilation, the compact clusters are less dense than in the previous cases (e.g., for $\sigma = 0.5$ the cluster density ρ is about $2/3$).

Using Eq. (5) we built the phase diagram shown in Fig. 7. Since $\langle \omega_i^c \rangle_c$ is proportional to $\ell^{-\sigma}$, it increases upon a decrease in σ. On the other hand, the average $\langle \omega_i^a \rangle_c$ also increases, as a result of more compact particle displacements. The competition between averages results in a net increase in α with a decrease in σ. Similarly to the σ-CP the pair mean-field approximation also gives first- and second-order transitions, with the tricritical point given by

$$\zeta(\sigma_t) = 4\frac{1+a}{a}. \tag{17}$$

Again, from this equation it follows that $\sigma_t > 1$. The pair mean field predicts a critical line at $\alpha_c = 1/2$.

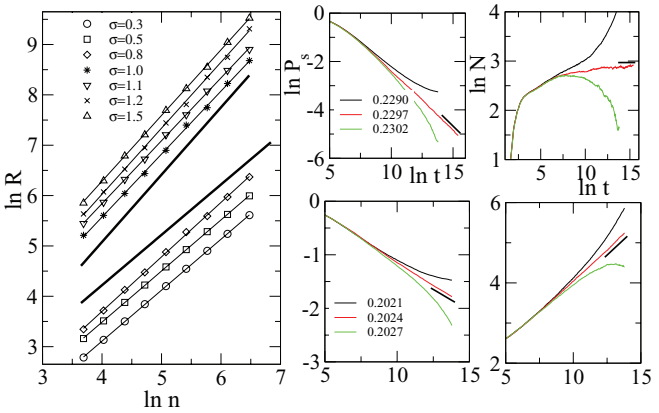

FIG. 6. (Color online) Log-log plot of R versus n for the long-range PAM and distinct values of σ. Straight lines have slopes of 1.337 04 (top) and 1 (bottom), respectively, and they have been shifted in order to avoid overlap. Right: Log-log plot of the time evolution of P_s (left) and N (right) for distinct α values for $\sigma = 0.3$ (top) and $\sigma = 1.2$ (bottom), respectively. Predicted asymptotic slopes are consistent with GI (top) and DP (bottom) values.

Now we consider the influence of the annihilation of three adjacent particles. This study is motivated by previous work [27,32] which shows that the inclusion of triplet annihilation causes large differences in the phase diagram, compared with single and pair annihilations. The transition rate ω_i^a is then given by

$$\omega_i^a = \eta_{i-1} \eta_i \eta_{i+1}, \tag{18}$$

and particles are created as in the σ-CP. In the conserved ensemble, Eq. (4) is used to calculate $\bar{\alpha}$ for $k = 3$. The short-range case ($a = 0$) has been extensively studied in Refs. [27, 32], where a continuous phase transition belonging to the DP universality class takes place at $\alpha_c = 0.148\,98(5)$. In Figs. 8 and 9, we plot the average cluster size R versus n and the phase diagram for different values of σ. As in previous cases, the phase transition is second order for $\sigma > 1$, becoming first order for $0 < \sigma < 1$. The crossover between continuous and discontinuous takes place between 0.8 and 1.1. As an effect

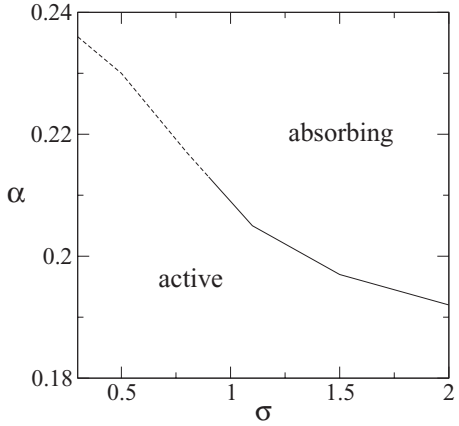

FIG. 7. Parameter α versus σ for the long-range PAM. Solid and dashed lines denote second- and first-order transitions, respectively.

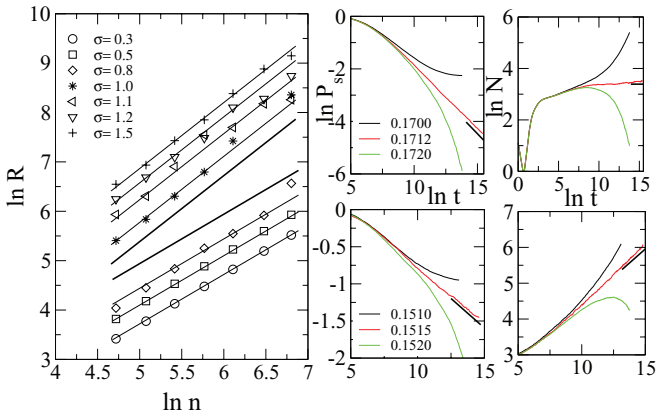

FIG. 8. (Color online) A log-log plot of R versus n for the long-range TAM and distinct values of σ. Straight lines have slopes of 1.337 (top) and 1 (bottom), respectively, and they have been shifted in order to avoid overlapping. Right: Log-log plots of the time evolution of P_s (left) and N (right) for distinct values of α for $\sigma = 0.3$ (top) and $\sigma = 1.2$ (bottom), respectively. Predicted asymptotic slopes at the top and bottom are consistent with GI and DP values.

of the triplet annihilation, the compact clusters are less dense than in all previous cases (for $a = 2$).

Using the same procedure as adopted previously, we built the phase diagram shown in Fig. 7. The transition point α varies mildly with σ, as an effect of the simultaneous increase in $\langle\omega_i^c\rangle_c$ and $\langle\omega_i^a\rangle_c$ with a decrease in σ. For smaller a, the system also presents phase coexistence, although the crossover seems to occur for smaller σ compared with the case $a = 2$. For example, for $a = 0.1$ and $\sigma = 0.5$, the transition is second-order ocurring at $\alpha_c = 0.1503(1)$, whereas for $\sigma = 0.1$ the phase coexistence occurs at $\alpha_0 = 0.1554(2)$.

As in the previous cases, the pair mean-field approximation reproduces first- and second-order transitions, with a critical line and tricritical point occurring at $\alpha_c = 2/3$ and

$$\zeta(\sigma_t) = 9\frac{1+a}{a}, \tag{19}$$

respectively. Also, as in the previous cases, it follows that $\sigma_t > 1$. In summary, the existence of a discontinuous transition in both the PAM and the TAM for $0 < \sigma < 1$ indicates that pair and triplet annihilations do not provoke fluctuations strong enough to lead to the suppression of compact clusters.

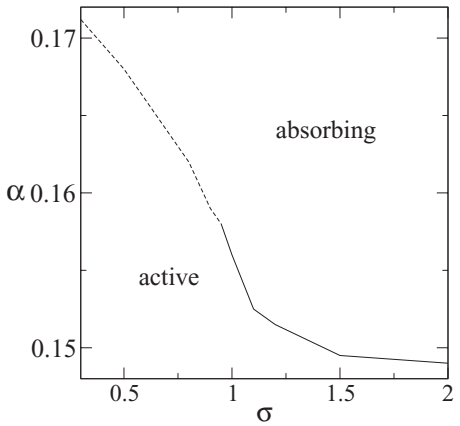

FIG. 9. Parameter α versus σ for the long-range TAM. Solid and dashed lines denote second- and first-order transitions, respectively.

C. Long-range pair contact process (σ-PCP)

In the PCP, only pairs of particles can be annihilated or create new particles. Unlike all previous models, any configuration devoid of pairs is absorbing and thus the PCP displays infinitely many absorbing states. The order parameter is the pair density ϕ instead of the particle density ρ. The PCP model has been extensively studied in the past [28,32], and despite the differences from all the previous models, its absorbing transition belongs to the DP universality class. Let p the probability of annihilating pairs of particles, the phase transition occurs at $p_c = 0.077\,090(5)$ [28,32]. The parameters p and α (used here) are related through the expression $p = \frac{\alpha}{\alpha+1}$.

The long-range version can be introduced similarly as in all previous cases. However, in order to investigate the role of infinitely absorbing states, we take two different cases. In the former, the activation rate is given by Eq. (15), implying that the distance ℓ is measured up to the nearest particle at the edge of an inactive island. The latter takes into account the distance up to the nearest pair, given by

$$\omega_i^c = \frac{1}{2}\sum_{\ell=1}^{\infty}\left(1+\frac{a}{\ell^\sigma}\right)\eta_{i-2}\eta_{i-1}\bar{\eta}_i\cdots\eta_{i+\ell}\eta_{i+\ell+1} + \frac{1}{2}\sum_{\ell=1}^{\infty}\left(1+\frac{a}{\ell^\sigma}\right)\eta_{i+2}\eta_{i+1}\bar{\eta}_i\cdots\eta_{i-\ell-1}\eta_{i-\ell}. \tag{20}$$

In both cases, the annihilation rate is given by Eq. (16).

Since the existence of infinite absorbing states makes the use of spreading simulations difficult, we adopt the procedure described in Sec. II, consisting of studying the time evolution of the pair density ϕ starting from a fully occupied lattice. In Fig. 10 we plot the decay of ϕ for different σ values by taking the first version. We focus the analysis on the case for $a = 2$ and low σ, in order to see the effect of strong long-range interactions. We see that for both cases, the decay of ϕ is algebraic at 0.188 05(5) ($\sigma = 0.5$) and 0.2365(1) ($\sigma = 0.1$), with exponents consistent with the DP value $\theta = 0.159\,464(6)$ [see short (black) lines]. This is the first evidence that the phase

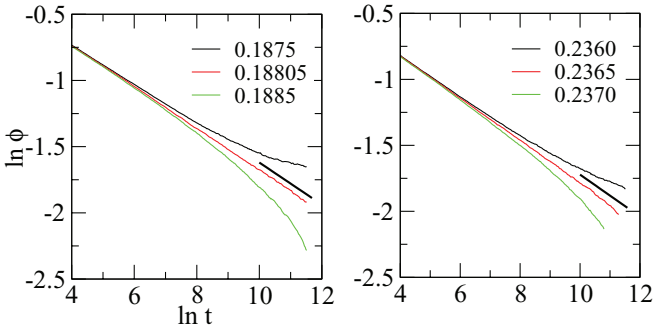

FIG. 10. (Color online) Log-log plots of the time evolution of the pair density ϕ starting from a fully occupied lattice for $\sigma = 0.5$ (left) and $\sigma = 0.1$ (right) for different α values. The short (black) lines by the middle curves have slopes consistent with 0.159 464(6).

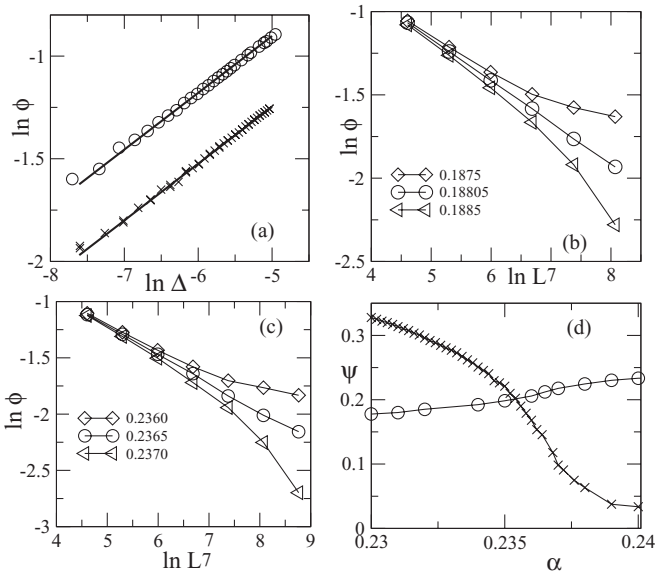

FIG. 11. (a) Log-log plot of ϕ versus $\Delta \equiv \alpha_c - \alpha$ for different σ values and $L = 3200$. Straight lines have slope 0.276 486. Log-log plots of ϕ versus L for (b) $\sigma = 0.5$ and (c) $\sigma = 0.1$. Straight lines have slope 0.252 0718. (d) Dependence of ψ on α, where $\psi = \phi$ (crosses) and $\psi = \rho - \phi$ (circles) for $\sigma = 0.1$.

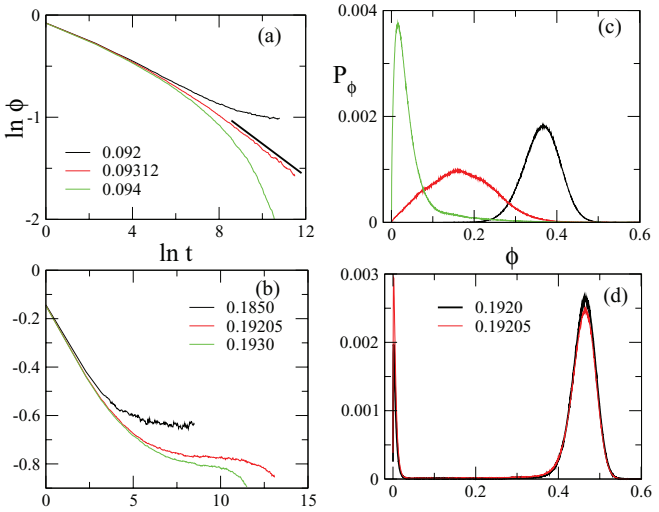

FIG. 12. (Color online) Log-log plot of the time decay of ϕ for $\sigma = 1.2$ (a) and for $\sigma = 0.1$ (b). Probability distribution P_ϕ vs ϕ for the σ-PCP and (c) $\sigma = 1.2$ and (d) $\sigma = 0.1$.

transition in such a case is second order for all σ values. In order to confirm this query, we also obtained static exponents, by performing steady numerical simulations. In the case of a continuous transition, ϕ will behave as $\phi \sim (\alpha_c - \alpha)^\beta$, where β is the associated critical exponent. In Fig. 11(a), we show a log-log plot of ϕ vs $\Delta \equiv \alpha_c - \alpha$ using the previous estimates for the α_c values. Note that both curves present slopes consistent with the DP value $\beta = 0.276\,486$ [bold (black) lines], confirming the second-order phase transition.

We also studied the dependence of the order parameter ϕ on the system size L. At criticality ϕ decays according to the power law $\phi \sim L^{-\beta/\nu_\perp}$, where $\nu_\perp$ is the critical exponent associated with the spatial length correlation. In fact, as shown in Figs. 11(b) and 11(c), for all α's (circles) ϕ also decays algebraically with L, with critical exponents consistent with the DP value of 0.252 0718 (solid lines). The above conclusions remain valid for larger a values. For example, for $a = 5$ and $\sigma = 0.5$, ϕ presents an algebraic decay at $\alpha_c = 0.3318(2)$, with a dynamic exponent consistent with the DP one. The absence of a discontinuous transition can be understood by inspecting the density of particles surrounded by at least one empty site $\rho - \phi$, which determines the strength of the long-range interaction in this case, as shown in Fig. 11(d) for $\sigma = 0.1$. The existence of infinitely absorbing states causes $\rho - \phi$ to change very slightly (close to the transition), implying that active states with low ϕ are not destabilized by the long-range interaction (even for low σ), and hence no abrupt change in ϕ occurs and the transition remains continuous.

It is worth mentioning that the absence of a discontinuous transition is not predicted by mean-field approximations. Upon taking two site correlations, the transition is discontinuous for $\sigma < \sigma_t$, with a tricritical point separating the first and second lines given by

$$\zeta(\sigma_t) = 2\frac{1+a}{a}. \tag{21}$$

Again, from this equation it follows that $\sigma_t > 1$. The pair mean field predicts a critical line at $\alpha_c = 1/4$.

In Fig. 12, we show the main results for the second version. In Figs. 12(a) and 12(b) we compare the time decay of ϕ for $a = 2$ with $\sigma = 1.2$ and $\sigma = 0.1$, respectively. In the former case, the slope at $\alpha_c = 0.093\,12$ agrees with the value 0.159 464(6), consistent with the emergence of second-order transitions for $\sigma > 1$. In contrast, the decay for $\sigma = 0.1$ is slightly different from that in the previous case, suggesting a first-order transition. The phase coexistence is confirmed by plotting the pair density probability distribution P_ϕ, as shown in Figs. 12(c) and 12(d) for $\sigma = 1.2$ and $\sigma = 0.1$, respectively. In fact, for $\sigma = 0.1$ P_ϕ is bimodal. Similar results for $\sigma = 0.5$ support a first-order transition for $0 < \sigma < 1$. This result can be understood by noting that in the present case ϕ plays a role similar to that of ρ in the σ-CP. The dynamics described by Eqs. (16) and (20) allows us to relate the σ-PCP and the σ-CP through the transformation $\eta_i \eta_{i+1} \to \eta'_i$. Since in the σ-CP states of low densities are disrupted by long-range interactions, a similar conclusion is valid for the σ-PCP. For the previous version, such an analogy cannot be drown, due to the dependence on one site occupied in the perimeter instead of two occupied sites. To close this section we remark that the coexistence line also seems to move toward larger σ values when a increases, although the crossover between the two regimes is broader than for the σ-CP.

V. CONCLUSION

First-order phase transitions into absorbing states require a robust mechanism of preventing the creation of particles in low-density regimes. Although there is strong evidence that they cannot occur in one-dimensional short-range CPs, a long-range counterpart reported by Ginelli *et al.* [25] revealed

such a possibility. Aimed at uncovering the fundamental mechanisms ruling long-range interactions as an effective mechanism of forming compact clusters, here we have investigated thoroughly a family of interaction rules. Our study includes seven contact models grouped in three distinct approaches. In the former, we have weakened long-range interactions and taken the competition between them with frequent short-range dynamics, whereas the latter replaces single by cluster interactions. All these results supported that a long-range small perturbation suffices to suppress low-density stable states, in the sense that the undertaken weakening long-range interactions are not sufficiently "strong" to destroy compact clusters. The mean-field approach gave us some insight to understand the above conclusions. Except for the σ-pair CP, the approximated expressions present a general structure, predicting a change in the phase transition for all a and σ. However, in contrast with numerical results, the critical lines present the same transition point α_c (for all $\sigma > \sigma_t$). Unlike previous cases, the presence of infinitely many absorbing states leads to novel and different scenarios, depending on the particle structures surrounding the edges of inactive sites. One of them predicts conclusions similar to those obtained with the previous models, whereas in the other version, the phase coexistence is destroyed. This result cannot be understood by the two-site mean-field theory, in which the phase transition also becomes first order for small values of σ. Although an increase in fluctuations may predict a second-order transition for small σ, we believe that, in the present case, a very large order of approximation would be required to reproduce a continuous transition. In summary, long-range interactions constitute an effective dynamics to create a discontinuous phase transition, even for the extreme limits undertaken here. As the final remark, we should mention that the effect of other dynamics such as diffusion and quenched disorder and its competition with long-range interactions should be investigated in a future contribution.

ACKNOWLEDGMENTS

We acknowledge Miguel A. Muñoz for a critical reading of the manuscript and useful suggestions. The financial support from the CNPQ is also acknowledged.

[1] J. Marro and R. Dickman, *Nonequilibrium Phase Transitions in Lattice Models* (Cambridge University Press, Cambridge, 1999).
[2] G. Grinstein and M. A. Muñoz, in *Fourth Granada Lectures in Computational Physics*, Lecture Notes in Physics, Vol. 493, edited by P. Garrido and J. Marro (Springer, Berlin, 1997), p. 223.
[3] T. E. Harris, Ann. Prob. **2**, 969 (1974).
[4] H. K. Janssen, Z. Phys. B **42**, 151 (1981); P. Grassberger, *ibid.* **47**, 365 (1982).
[5] M. A. Muñoz, in *Advances in Condensed Matter and Statistical Mechanics*, edited by E. Korutcheva and R. Cuerno (Nova Science Publ., Hauppauge, NY, 2003).
[6] G. Odor, Rev. Mod. Phys. **76**, 663 (2004).
[7] K. A. Takeuchi, M. Kuroda, H. Chaté, and M. Sano, Phys. Rev. Lett. **99**, 234503 (2007).
[8] See, for example, A. Lipowski, Phys. Rev. E **62**, 4401 (2000); H. Hinrichsen, *ibid.* **63**, 016109 (2000).
[9] S.-G. Lee and S. B. Lee, Phys. Rev. E **80**, 011106 (2009).
[10] C. E. Fiore and M. J. de Oliveira, Braz. J. Phys. **36**, 218 (2006).
[11] R. Dickman and T. Tomé, Phys. Rev. A **44**, 4833 (1991).
[12] C. E. Fiore and M. J. de Oliveira, Phys. Rev. E **70**, 046131 (2004).
[13] G. Cardozo and J. F. Fontanari, Eur. Phys. J. B **51**, 555 (2006).
[14] H. Hinrichsen, arXiv:cond-mat/0006212.
[15] S.-C. Park, Phys. Rev. E **80**, 061103 (2009).
[16] D. Vernon and M. Howard, Phys. Rev. E **63**, 041116 (2001).
[17] D. C. Vernon, Phys. Rev. E **68**, 041103 (2003).
[18] D. Mollison, J. R. Stat. Soc. Ser. B (Methodol) **39**, 283 (1977).
[19] P. Grassberger, in *Fractals in Physics*, edited by L. Pietronero and E. Tosatti (Elsevier, New York, 1986).
[20] H. K. Janssen, K. Oerding, F. van Wijland, and H. J. Hilhorst, Eur. Phys. J. B **7**, 137 (1999).
[21] H. Hinrichsen and M. Howard, Eur. J. Phys. B **7**, 635 (1999).
[22] C. J. Tessone, M. Cencini, and A. Torcini, Phys. Rev. Lett. **97**, 224101 (2006).
[23] F. Ginelli, H. Hinrichsen, R. Livi, D. Mukamel, and A. Torcini, J. Stat. Mech. (2006) P08008.
[24] H. Hinrichsen, J. Stat. Mech. (2007) P07006.
[25] F. Ginelli, H. Hinrichsen, R. Livi, D. Mukamel, and A. Politi, Phys. Rev. E **71**, 026121 (2005).
[26] C. E. Fiore and M. J. de Oliveira, Phys. Rev. E **76**, 041103 (2007).
[27] R. Dickman, Phys. Rev. B **40**, 7005 (1989).
[28] I. Jensen, Phys. Rev. Lett. **70**, 1465 (1993).
[29] T. Tomé and M. J. de Oliveira, Phys. Rev. Lett. **86**, 5643 (2001).
[30] H. J. Hilhorst and F. van Wijland, Phys. Rev. E **65**, 035103(R) (2002).
[31] M. J. de Oliveira, Phys. Rev. E **67**, 027104 (2003).
[32] C. E. Fiore and M. J. de Oliveira, Phys. Rev. E **72**, 046137 (2005).
[33] I. Jensen and R. Dickman, Phys. Rev. E **48**, 1710 (1993).
[34] M. A. Muñoz, G. Grinstein, R. Dickman, and R. Livi, Phys. Rev. Lett. **76**, 451 (1995).
[35] M. A. Muñoz, G. Grinstein, R. Dickman, and R. Livi, Physica D **103**, 485 (1997).
[36] M. A. Muñoz, G. Grinstein, and R. Dickman, J. Stat. Phys. **91**, 541 (1998).
[37] H.-M. Bröker and P. Grassberger, Physica A **267**, 453 (1999).
[38] T. Vicsek, *Fractal Growth Phenomena*, 2nd ed. (World Scientific, Singapore, 1992).